Using Folded Open-Loop Ring Resonator to Design a Common-Mode Suppression and Frequency Adjustable Balun-Bandpass Filter

Chia-Mao Chen [1], Shoou-Jinn Chang [2], Jia-Chun Zheng [3], Jian-Chiun Liou [4], and Cheng-Fu Yang*[5]

[1] Department of Electrical Engineering
National Cheng Kung University, Tainan 701, Taiwan
jmchen0813@gmail.com

[2] Institute of Microelectronics and the Department of Electrical Engineering
Advanced Optoelectronic Technology Center, Center for Micro/Nano Science and Technology
National Cheng Kung University, Tainan 701, Taiwan
changsj@mail.ncku.edu.tw

[3] School of Information Engineering, Jimei University, Xiamen 361021, China.
jchzheng@jmu.edu.cn

[4] Department of Electronic Engineering
National Kaohsiung University of Applied Sciences, Kaohsiung 807, Taiwan
jcliou@kuas.edu.tw

[5]*Department of Chemical and Materials Engineering
National University of Kaohsiung, Kaohsiung 811, Taiwan
cfyang@nuk.edu.tw

Abstract **─** A compact and simple balun-bandpass filter was investigated by using a pair of half-wavelength open-loop ring resonators (OLRRs) and two microstrip lines. The balun-bandpass filter could be designed easily with a different center frequency by changing the path length of OLLRRs. The design methodology was adopted based on EM simulation to obtain these optimally designed parameters of the OLRRs, and microstrip lines and the filters were fabricated on FR4 substrate. The filters with the frequencies of 2.6 GHz and 5.2 GHz were designed to prove the characteristic of frequency adjustable and they were fabricated with the properties of wide bandwidth and low insertion loss. The balun-bandpass filters presented an excellent in-band balanced performance with common-mode rejection ratio over than 40 dB and 34 dB in the passbands of 2.6 GHz and 5.2 GHz, respectively. Good correlation was seen between simulation and measurement, and the result showed that first run pass had been achieved in the majority of our design.

Index Terms **─** Balanced impedance, balun-bandpass filter, frequency adjustable, open-loop ring resonators (OLRRs).

I. INTRODUCTION

As compared with conventional single-ended circuits balanced circuit has higher immunity to the environmental noise. Therefore, many devices have been designed in balanced topologies, such as low-noise amplifiers, mixers, oscillators, power amplifiers, filters, and antennas. Baluns, which are used as an interface device, are necessary for the conversion between balanced devices and unbalanced ones. A modern communication system needs a compact and low-cost RF module; thus, a device with multifunction is desired. The balun diplexer or filter are such devices that they are not only with a filtering function, but they are also a balun converting between balanced singles and unbalanced ones. Recently, several methods have been developed to design the balun filters [1-6]. For multi-service and multi-band communication systems, the diplexer is an essential component that is built by two bandpass filters (BPFs) with different passband frequencies [7-9].

In the present study, a generalized methodology for designing a novel and simple single passband balun BPF was investigated. The low-loss balun BPF was designed by using a folded open-loop ring resonators

Submitted On: June 24, 2015
Accepted On: December 6, 2015

(OLRRs) with equal physical dimensions to couple two microstrip lines, as Fig. 1 shows. The OLRRs were placed between two microstrip lines and had a perimeter of about a half wavelength of the designed resonant frequency. The OLRRs had its maximum electric field density near the open ends of the line and had its maximum magnetic field density around the center valley of the microstrip line. The resonant frequency was adjustable via the length of the OLRRs to provide a high-performance passband response. We would show that a compact microstrip balun filter was designed with high isolation and CM suppression. Based on the proposed idea, two filters with the central frequencies of 2.6 GHz and 5.2 GHz for WLAN and WiMAX applications were implemented by changing the different lengths of OLRRs. Finally, we fabricated two high-performance balun BPFs on FR4 substrates, and the predicted results were well confirmed by the measured results. We would show that the proposed balun BPFs had low insertion loss, a wide bandwidth, transmission zeros, and simple structure, and no extra circuit was needed to suppress the harmonic, respectively.

II. DESIGN METHODOLOGY

The balun BPF with central frequency of 2.6 GHz for LTE band system was first designed to prove the proposed idea accomplished by using OLRRs and the discriminating coupling technique [10-13]. When the discriminating coupling technology is used, the second harmonics of coupled-line BPFs are rejected without requiring any extra circuit and degrading in-band performance and the effect of common-mode suppression will be achieved [9]. The coupled structures resulted from different orientations of a pair of open-loop ring resonators (OLRRs) and from the microstrip lines, which were separated by a spacing S_{OLRR}, as Fig. 1 shows. Each of the OLRRs essentially acted as a folded half-wavelength resonator. Any coupling in those structures was the proximity coupling; basically, the coupling was formed through fringe fields. The nature and the extent of the fringe fields determined the nature and the strength of the coupling effect. At the resonance of fundamental mode, each of the OLRRs had the maximum electric field density at the side with an open gap (g_{OLRR}) and the maximum magnetic field density at the opposite side. Therefore, the electric coupling could be obtained if the open sides of two coupled resonators were proximately placed.

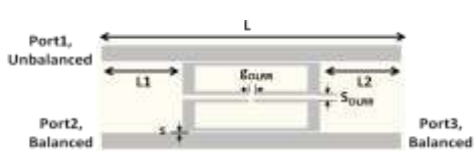

Fig. 1. Proposed balun-bandpass filter (BPF) based on OLRRs.

To obtain the maximum magnetic coupling, the center valley of the OLRRs should be positioned in the proper location along the microstrip lines at which the maximum magnetic field intensity existed. For the transverse electromagnetic (TEM) field structure, both the electric and magnetic field vectors lied in the transverse plane, which was perpendicular to the uniform propagation axis. Under the assumptions of the TEM mode of propagation and a lossless line, the fields $\vec{E}$ and $\vec{H}$ were uniquely related to voltage and current, respectively. Based on transmission line theory, the magnitudes of voltage and current on the microstrip lines could be expressed in terms of the incident wave and the reflection coefficient for an open-circuited line as:

$$|V(z)| = |V_0^+| |1 + e^{j(\theta - 2\beta l)}|, \quad (1)$$

$$|I(z)| = \frac{|V_0^+|}{Z_0} |1 - e^{j(\theta - 2\beta l)}|, \quad (2)$$

where $l = -z$ is measured away from the load at $z = 0$, and θ is the phase of the reflection coefficient. When θ-2 βd has a magnitude of zero or any multiple of 2π radian, voltage in (1) is at its maximum magnitude and current in (2) is at its minimum magnitude, respectively. Figure 2 depicts the normalized voltage/current distributions of the open-ended transmission lines. At a distance of a quarter wavelength from the receiving end, the voltage becomes zero while the current is at its maximum. If the line has a value of half wavelength, the current distribution near the center of the transmission line is at its maximum, and high magnetic coupling results from a high conduction current. Once the point of I_{max} is found, the point of H_{max} can be easily determined. When odd-mode excitation is applied to balanced port, there is a voltage null at the center of the microstrip line, the voltage/current distributions are shown in Fig. 3.

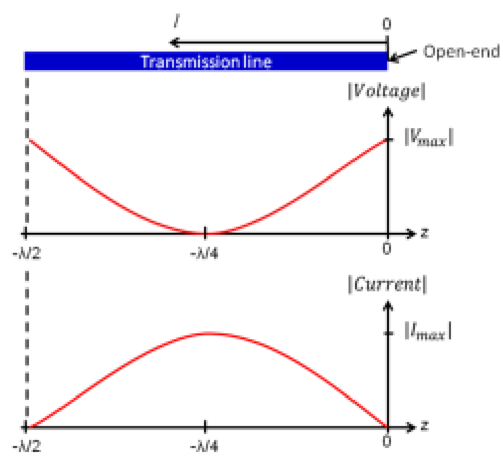

Fig. 2. Voltage and current distribution in microstrip line terminated at open end.

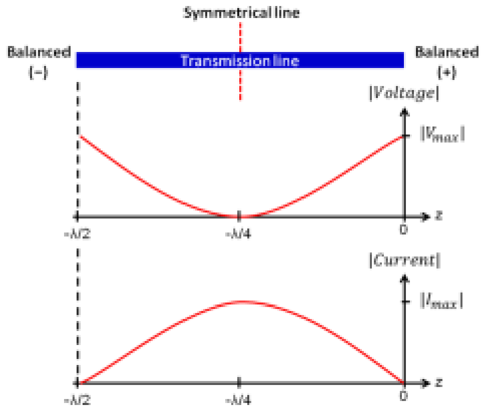

Fig. 3. Voltage and current distributions of the odd-mode.

To demonstrate the proposed structure was available, balun BPF was designed using OLRRs to couple the microstrip transmission lines. After the designed balun BPFs were simulated using the HFSS simulator with loss factors (conductor loss and dielectric loss) included in the simulated response to find the optimal parameters. In order to characterize the balance characteristic of the balun BPFs, the mode conversion between the unbalanced three-port network and the unbalanced-to-balanced two-port network was applied to obtain the single-ended to differential-mode and common-mode -parameters [7,14]:

$$S_{ss11}= S_{11}, \quad (3)$$

$$S_{ds21}= (S_{21} - S_{31})/(2)^{1/2}, \quad (4)$$

$$S_{cs21}= (S_{21} + S_{31})/(2)^{1/2}, \quad (5)$$

where S_{ss11} is the return loss at the unbalanced port 1, S_{ds21} is the two-port S-parameters from the unbalanced port 1 to differential-mode balanced port 2, and S_{cs21} is the two-port S-parameters from the unbalanced port 1 to common-mode balanced port 2, respectively.

III. DESIGN OF BALUN-BANDPASS FILTERS

The balun BPFs were designed on a pair of half-wavelength OLRRs with the center frequencies of 2.6 GHz and 5.2 GHz by changing the length of OLRRs. The simulated results shown in Fig. 4, Fig. 5 and Fig. 6 for balun BPF with center frequency of 2.6 GHz was used to prove that the proposed idea could be used to design the balun BPFs with common-mode suppression. Electric coupling was obtained if the open sides of the coupled resonators were placed near each other, and magnetic coupling was obtained if the sides with the maximum magnetic field of the coupled resonators were placed near each other. The coupling spacing *s* between the main microstrip line and OLRRs was 0.2 mm and the spacing S_{OLRR} between two resonators was 0.61 mm. Figure 4 and Fig. 5 illustrate the effect of different S_{OLRR} and *s* on the frequency response of the balun filter by full-wave simulated.

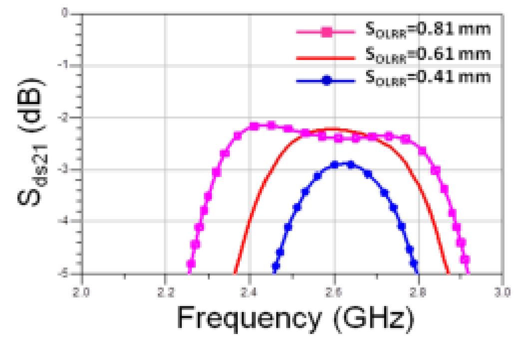

(a)

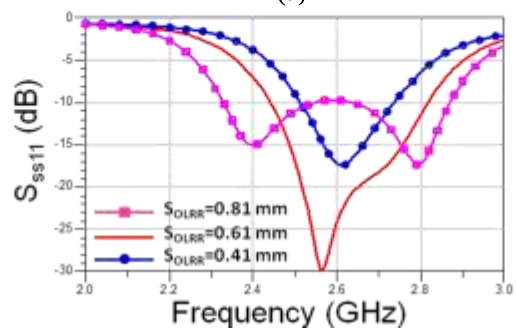

(b)

Fig. 4. Simulation results of various gap S_{OLRR} for designed balun BPF at 2.6 GHz. (a) Differential-mode response, S_{ds21}. (b) Differential-mode response, S_{ss11}.

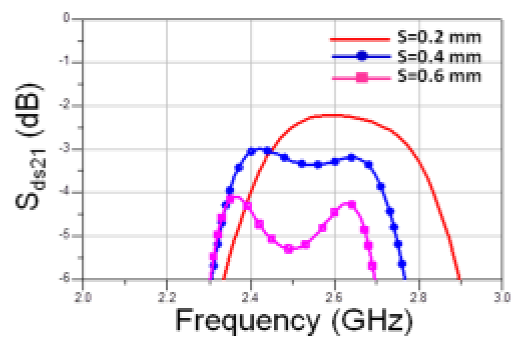

(a)

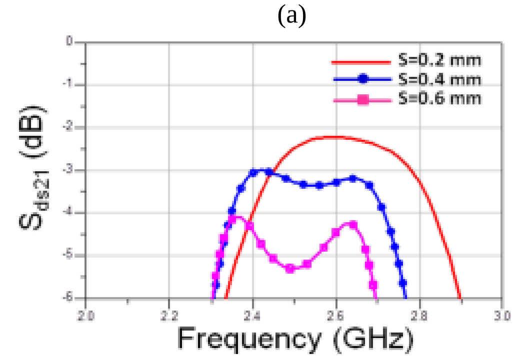

(b)

Fig. 5. Simulation results of various gap *s* for designed balun BPF at 2.6 GHz. (a) Differential-mode response, S_{ds21}. (b) Differential-mode response, S_{ss11}.

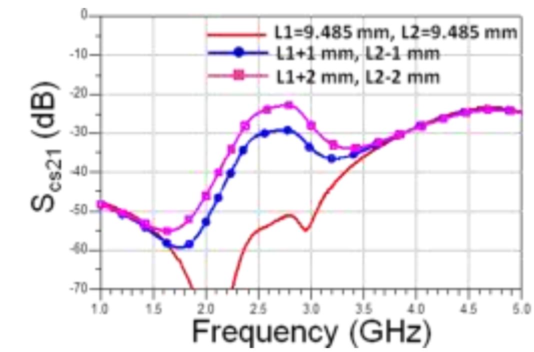

(a)

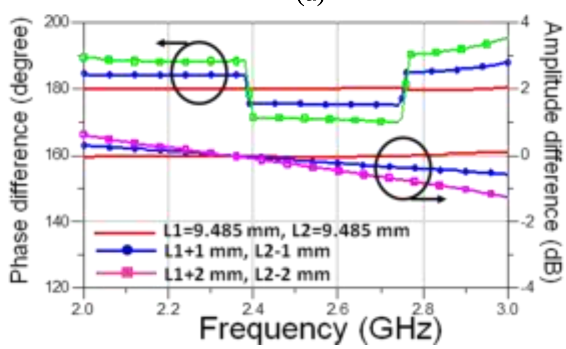

(b)

Fig. 6 Simulation results of different orientations for OLRRs for 2.6 GHz designed. (a) Common-mode response, S_{ds21}. (b) Phase/amplitude difference.

The results in Fig. 4 show that as the coupling spacing *s* decreased the two resonant peaks moved outwards and the trough in the middle deepens, which implies an increase in the coupling. The coupling of the coupled line stricture in Fig. 5 could be found from the coupling gap *s*. A smaller gap resulted in a stronger I/O coupling or a smaller external quality factor of the resonator. To further demonstrate the importance of optimal locations for balun characteristic, Fig. 6 shows a comparison of passband responses of different orientations for OLRRs. The simulation result of the designed balun BPF shows good match in input impedance, good amplitude, and phase balance between two output ports, and a wide passband, respectively.

The balun BPF using OLRRs was fabricated on an FR4 substrate with a relative permittivity of 4.4 and a thickness between the two electrodes was 1.0 mm. The dimension for the proposed 2.6 GHz balun BPF was 35 mm × 13.23 mm, as shown in Fig. 7 (a), and the photograph of the fabricated balun BPF is shown in Fig. 7 (b). The dimension for the proposed 5.2 GHz balun BPF was 17 mm × 13.43 mm, as shown in Fig. 8 (a), and the photograph of the fabricated balun BPF is shown in Fig. 8 (b). Measurements were carried out using an Agilent N5071C network analyzer.

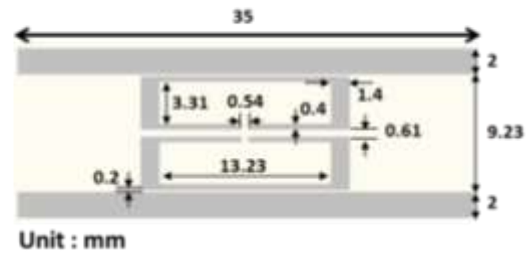

(a)

(b)

Fig. 7. (a) Layout pattern and (b) photograph of the designed balun BPF with central frequency of 2.6 GHz.

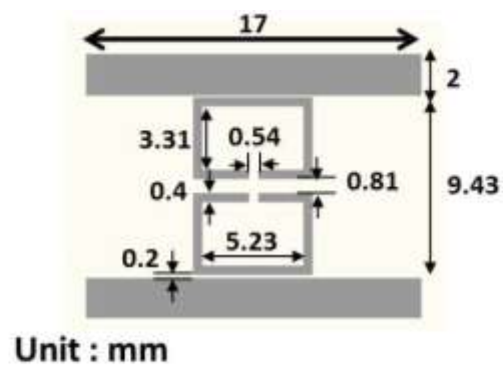

(a)

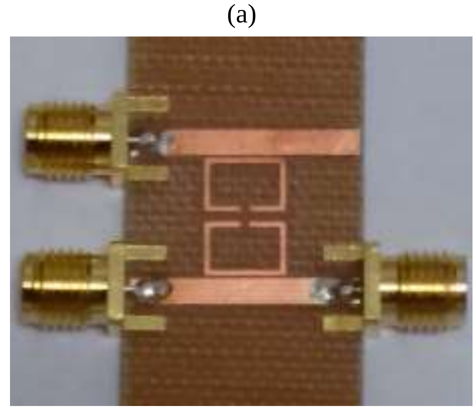

(b)

Fig. 8. (a) Layout pattern and (b) photograph of the designed balun BPF with central frequency of 5.2 GHz.

Figures 9 (a) and 9 (b) show the full-wave simulated and measured results of the S-parameters and phase/ amplitude differences for the circuit at low band. For differential-mode operation, the passband in Fig. 9 was centered at 2.6 GHz with 1 dB bandwidth of 240 MHz, or 9.23% and the minimum insertion loss including SMA connectors was measured to be 2.46 dB. Figure 9 (b) shows that the amplitude difference between S_{21} and S_{31} was below 0.2 dB and the phase difference between S_{21} and S_{31} was within 180 $\pm$ 2° for low band. Both the simulated and measured S_{cs21} values were smaller than 40 dB within operating band of the designed 2.6 GHz balun BPF, which demonstrates the effect of good common-mode suppression at the differential output port. Figures 10 (a) and 10 (b) show those for the circuit at high band, respectively. The passband in Fig. 10 was centered at 5.44 GHz with 1 dB bandwidth of 280 MHz, or 5.15% with minimum insertion loss including SMA connectors at 3.13 dB. The simulated and measured S_{cs21} values were smaller than 34 dB with in operating bands of the designed 5.2 GHz balun BPF. Figure 10 (b) show that the amplitude difference between S_{21} and S_{31} was below 0.3 dB and the phase difference between S_{21} and S_{31} was within 180 $\pm$ 3° for high band. The little differences between the simulated and measured results are mainly caused by the fabrication error (circuit etching), the SMA connector, and numerical error.

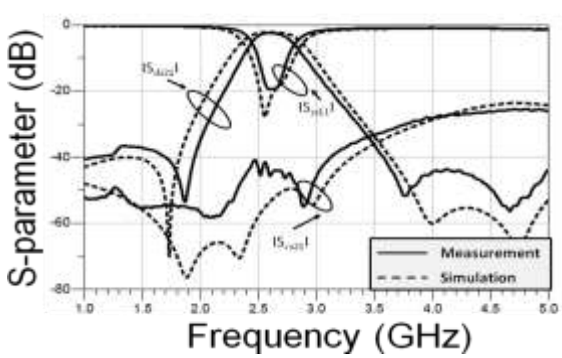

(a)

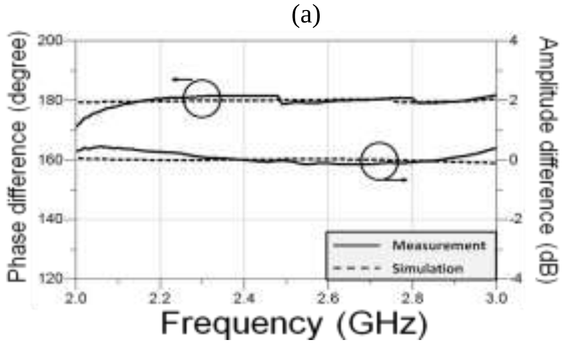

(b)

Fig. 9. Measured: (a) S-parameters and (b) phase/ amplitude difference of the designed balun BPF with central frequency of 2.6 GHz.

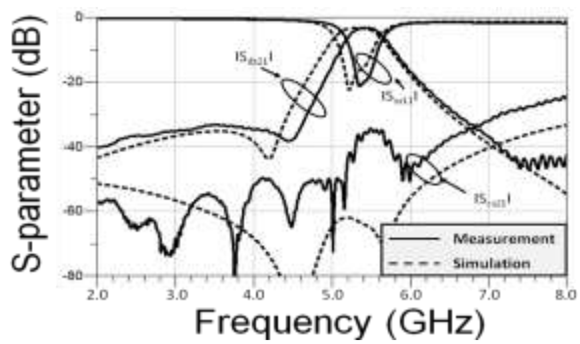

(a)

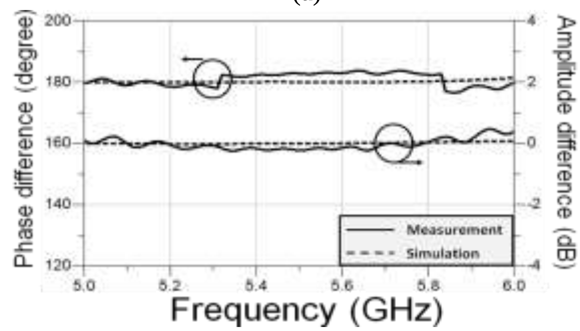

(b)

Fig. 10. Measured: (a) S-parameters and (b) phase/ amplitude difference of the designed balun BPF with central frequency of 5.2 GHz.

VI. CONCLUSION

We proposed a simple and effective method to design the microstrip balun BPFs with the properties of common-mode suppression and central frequency adjustable. The dimension for the proposed 2.6 GHz balun BPF was 35 mm × 13.23 mm and for the proposed 5.2 GHz balun BPF was 17 mm × 13.43 mm, respectively. Both the simulated and measured S_{cs21} values were smaller than 40 dB within operating band of designed 2.6 GHz balun BPF and smaller than smaller than 34 dB within operating band of designed 5.2 GHz balun BPF, which demonstrates good common-mode suppression at the differential output port. The fabricated 2.6 (5.44) GHz BPF had the properties of with 1 dB (1 dB) bandwidth of 230 MHz or 8.85% (280 MHz or 5.15%), minimum insertion loss including SMA connectors of 2.6 dB (3.13 dB), and the S_{ds21} value values were smaller than 40 dB (34 dB) within operating band. The amplitude difference between S_{21} and S_{31} was below 0.2 dB (0.3 dB) and the phase difference between S_{21} and S_{31} was within 180 $\pm$ 2° (180 $\pm$ 3°) at operating band. In this study, the designed and fabricated balun BPFs not only possessed good bandpass characteristics but they also provided great balun performance.

ACKNOWLEDGMENT

The authors acknowledge financial supports of NSC

101-2221-E-005-065, NSC 102-2622-E-390-002-CC3, and NSC 102-2221-E-390-027. This work was also supported by Fujian Nature Science Foundation under Grant No. 2013J01203 and Key Project of Science and Technology Project of Fujian Province in China under Grant No. 2014H0036.

REFERENCES

[1] M. Tamura, T. Ishizaki, and M. Hoft, "Design and analysis of vertical split ring resonator and its application to unbalanced-balanced filter," *IEEE Trans. Microw. Theory Tech*., vol. 58, no. 1, pp. 157-164, 2010.

[2] L. K. Yeng and K. L. Wu, "An LTCC balanced-to-unbalanced extracted-pole bandpass filter with complex load," *IEEE Trans. Microw. Theory Tech*., vol. 54, no. 4, pp. 1512-1518, 2006.

[3] E. Y. Jung and H. Y. Hwang, "A balun-BPF using a dual mode ring resonator," *IEEE Microw. Wireless Compon. Lett*., vol. 17, no. 9, pp. 652-654, 2007.

[4] S. J. Kang and H. Y. Hwang, "Ring-balun-bandpass filter with harmonic suppression," *IET Microw. Antennas Propag*., vol. 4, no. 11, pp. 1847-1854, 2010.

[5] L. H. Zhou, H. Tang, J. X. Chen, and Z.-H. Bao, "Tunable filtering balun with enhanced stopband rejection," *Electron. Lett*., vol. 48, no. 14, 2012.

[6] G. S. Huang and C. H. Chen, "Dual-band balun bandpass filter with hybrid structure," *IEEE Microw. Wireless Compon. Lett*., vol. 21, no. 7, pp. 356-358, 2011.

[7] Q. Xue, J. Shi, and J. X. Chen, "Unbalanced-to-balanced and balanced-to-unbalanced diplexer with high selectivity and common-mode suppression," *IEEE Trans. Microw. Theory Tech*., vol. 59, no. 11, pp. 2848-2855, 2011.

[8] Z. H. Bao, J. X. Chen, E. H. Lim, and Q. Xue, "Compact microstrip diplexer with differential outputs," *Electron. Lett*., vol. 46, no. 11, pp. 766-768, 2010.

[9] Y. X. Ji and J. Xu, "Compact BPF and diplexer using capacitively loaded $\lambda/4$ shorted meander line resonator," *J. Electromagnet. Waves Appl*., vol. 28, no. 1, pp. 112-118, 2014.

[10] C. Y. Chen and C. Y. Hsu, "A simple and effective method for microstrip dual-band filters design," *IEEE Microw. Wireless Compon. Lett*., vol. 16, no. 5, pp. 246-248, May 2006.

[11] J. S. Hong, *Microstrip Filters for RF/Microwave Applications*, 2nd edition, Wiley, New York, 2011.

[12] X. Y. Zhang and Q. Xue, "Harmonic-suppressed bandpass filter based on discriminating coupling," *IEEE Microw. Wireless Compon. Lett*., vol. 19, no. 11, pp. 695-697, 2009.

[13] Y. C. Li, X. Y. Zhang, and Q. Xue, "Bandpass filter using discriminating coupling for extended out-of-band suppression," *IEEE Microw. Wireless Compon. Lett*. vol. 20, no. 7, pp. 369-371, 2010.

[14] W. R. Eisenstadt, R. Stengel, and B. M. Thompson, *Microwave Differential Circuit Design Using Mixed-Mode S-Parameters*, Boston, MA, USA, 2006.

Chia-Mao Chen was born in Kaohsiung, Taiwan, on August 13, 1979. He received the B.S. from Kao Yuan University, Luzhu, Taiwan, in 2002, the M.S. degree from National Kaohsiung University of Applied Science (KUAS), Kaohsiung, Taiwan, in 2004, and is currently working toward the Ph.D. degree at National Cheng Kung University (NCKU), Tainan, Taiwan. His current research interests include design of antennas and microwave circuits.

Shoou-Jinn Chang (M'06–SM'10) was born in Taipei, Taiwan, on January 17, 1961. He received the B.S. degree from National Cheng Kung University (NCKU), Tainan, Taiwan, in 1983, the M.S. degree from the State University of New York, Stony Brook, NY, USA, in 1985, and the Ph.D. degree from the University of California, Los Angeles, USA, in 1989, all in Electrical Engineering. From 1989 to 1992, he was a Research Scientist with Nippon Telegraph and Telephone Basic Research Laboratories, Musashino, Tokyo, Japan. He joined the Department of Electrical Engineering, NCKU, in 1992 as an Associate Professor, where he was promoted to Full Professor in 1998. He is currently the Deputy Director of the Advanced Optoelectronic Technology Center, NCKU. From August to September 2001, he was a Visiting Scholar with the Institute of Microstructural Science, National Research Council, Canada; from August to September 2002, he was a Visiting Scholar with the Institute of Physics, Stuttgart University, Stuttgart, Germany; and from July to September 2005, he was a Visiting Scholar with the Faculty of Engineering, Waseda University, Tokyo. He is also an Honorary Professor with the Changchun University of Science and Technology, China. His current research interests include semiconductor physics, optoelectronic devices, and nanotechnology. Chang received the Outstanding Research Award from the National Science Council, Taiwan, in 2004. He is a Fellow of the Optical Society of America and the International Society for Optical Engineers.

Jia-Chun Zheng was born on June 9, 1965. Since 2000, Zheng was an Associate Professor and was a Vice President from 2011 at the School of Information Engineering, Jimei University, and he was also a Postgraduate Tutor from 2008. His current research interests are focused on sea transportation information system, signal processing, underwater acoustic communication, wireless sensor network. So far, his achievements have been awarded as the third prize of Scientific and Technological Progress in Xiamen, two utility model patents, and two software copyrights. He has published more than 20 papers and edited a textbook.

Jian-Chiun Liou was born in Taiwan on Oct. 18, 1974. He received a Ph.D. degree from the Institute of Nanoengineering and Microsystems, National Tsing Hua University, Hsinchu, Taiwan, in 2009. He joined the Printing Technology Development and Manufacturing Section of the Optoelectronics and Systems Laboratories at the Industrial Technology Research Institute (ITRI), Hsinchu, in 1999. In August 2014, he has joined the faculty of the National Kaohsiung University of Applied Sciences (KUAS). Currently, he is a Professor of Electronic Engineering department at the KUAS. He is a holder of 71 patents, and has written more than 28 SCI Journal papers and 38 conference technical papers on MEMS, optical-N/MEMS, and display-related and micro-/nanofluidics related fields. Liou was the recipient of the following honors: ITRI/OES Research Achievement Award (2004), ITRI Research Paper Publication Award (2004), ITRI/EOL Research Achievement Award (Individual person Award, 2005), ITRI Paper Awards (2012), ITRI/EOL Outstanding Advanced Research Silver Award (2013), International Inventor Prize (2014), Nation Academic Award (2014). He has also been a consultant to three Taiwanese companies.

Cheng-Fu Yang was born in Taiwan on July 12, 1964. After graduating in the “Department of Electrical Engineering” from Cheng Kung University in 1986, Yang also gained his Master and Ph.D. in 1988 and 1993 from the “Department of Electrical Engineering” of Cheng Kung University. After obtaining the Ph.D. degree, Yang entered academic life in 1993, first at the “Department of Electronic Engineering, Chinese Air Force Academy”, and since February 2000 as a Professor at the Chinese Air Force Academy, Taiwan. In February 2004, had joined the faculty of the National University of Kaohsiung (NUK) and he is a Professor in the Department of Chemical and Materials Engineering. He was the first one to get the Distinguished Professor in NUK. He was the Fellow of “Taiwanese Institute of Knowledge Innovation” (TIKI) on Oct, 2014 and he was the Fellow of “The Institution of Engineering and Technology” (IET) on May, 2015. His current research interests are focused on fine ceramics, microwave ceramics, dielectric thin films, optical materials, transparent conducting oxides, solar cell materials, microwave antennas, and microstrip filters. So far, he has published more than 175 SCI journal papers and more than 130 EI journal papers, and he also has published more than 260 domestic and international conference papers.